CryoModel: a cryostat thermal performance simulation tool

D. Pérez Caparrós / TE-MSC

Summary

In the design process of cryostats for accelerators equipment (magnets or RF cavities), it is of interest to estimate downtime for intervention. For this purpose, it is necessary to understand the temperature transients of the accelerator components during warm-up and cool-down processes. In this report, a mathematical model and a simulation tool to study the main heat transfer phenomena of a generic horizontal cryostat (radiation, with or without multilayer insulation system, actively cooled thermal shielding, thermal conduction through supporting systems, etc.) is presented. The thermal model and simulator have been benchmarked on experimental data from transients of the Large Hadron Collider (LHC). The presented tool is now being used to estimate the warm-up time needed for machine intervention in case of replacement of one cryomodule of the Superconducting Proton Linear accelerator (SPL).

1 Introduction

1.1 Generic cryogenic equipment for accelerators

Accelerator cryostats are designed to provide a stable mechanical support for the cold mass and to limit the heat in-leaks from the environment to a level that matches the tight heat load budget. They must withstand as well thermal transients, such as rapid cool-down and warm-up.

The major components of a generic cryostat that contribute to the properly insulation of the cold mass are the vacuum vessel, thermal shield, multilayer insulation system, and supporting system [12].

1.1.1 Vacuum vessel

The vacuum vessel, ordinarily at room temperature, maintains the insulating vacuum environment for the cold mass and other internal piping. It is usually built from rolled and welded sections of carbon steel pipe (sometimes stainless steel too) connected at heavier-walled reinforcing sections. The reinforcing sections are coincident with the internal supports and transfer the weight and any mechanical loads to ground.

1.1.2 Thermal shield

The thermal radiation shield is the next layer from the vacuum vessel; it surrounds the entire cold assembly. Its purpose is to intercept the heat radiating from the inner surface of the vacuum vessel, at room temperature, and most of the heat conducted through the supporting system before it reaches the cold mass. It is normally built in copper or aluminium and it is actively cooled by a cryogenic line to extract the intercepted heat.

1.1.3 Multilayer insulation system (MLI)

MultiLayer Insulation system (MLI) is made in blankets consisting of several low emittance shields, usually between 20 and 30 per cm of insulation thickness, separated by thin non-conducting spacers. These shields are generally made in plastic (Mylar or Kapton), which has a low thermal conductivity, and are coated with vacuum-deposited aluminium or gold. Spacers between shields are usually made in nylon or polyester and they are commonly produced in net form (tulle) with high porosity.

Heat transfer through MLI is mainly due to three thermally coupled heat transfer mechanisms: radiation, solid conduction through spacers, and residual gas conduction. These mechanisms depend on the MLI material thermal properties (thermal emissivity and conductivity), the blanket shields density, and vacuum conditions. Practical installation of MLI can also have a big impact on its thermal performance.

The thermal shield and the cold mass are covered with MLI blankets. Below 20 K, aluminized Mylar is almost transparent to infrared radiation. MLI blanket on the cold mass is used as protection from residual gas conduction at times of degraded insulation vacuum.

1.1.4 Supporting system

Supporting system must guarantee accurate and stable positioning of the cold mass within the cryostat. The supports, which are in direct contact with the cold mass, are built with materials that provide high stiffness and low thermal conductivity to limit conduction heat in-leaks from the vacuum vessel at room temperature [13]. Each support post normally mounts several heat intercepts at intermediate locations of the column, which may be actively cooled by cryogenic lines.

1.2 Thermal transients: warm-up and cool-down

Thermal transients are standard operating modes in accelerators [22]. They need to be studied to assess thermal gradients in the cold mass during cool-down and warm-up and thus verify design calculations.

The cool-down transient mode consists on cooling the cold mass from ambient temperature to the cryogenic operation temperature. It is usually carried out by forced circulation of gaseous helium.

The warm-up is the process of warming the cold mass from cryogenic temperature to ambient temperature and it is normally also carried out by forced circulation of gaseous helium. A natural warm-up occurs when there is no helium supply in the cryogenics lines, so there is a natural temperature drift of helium bath.

2 Modeling cryostat thermal performance

The evolution with time of the temperature in a cryostat has been simulated using a simplified one-dimensional radial model of a generic cryostat (see Fig. 1). This model consists of a cold mass, a thermal shield and a vacuum vessel. Blankets of MLI with different number of layers thermally insulate the thermal shield and the cold mass.

2.1 Heat transfer processes

An efficient thermal insulation system is essential in the design of any cryostat. It is important to reduce as much as possible the cryostat heat in-leaks from the environment. Radiation, convection, solid conduction and conduction in residual gas are the main heat transfer mechanisms that contribute to these heat in-leaks.
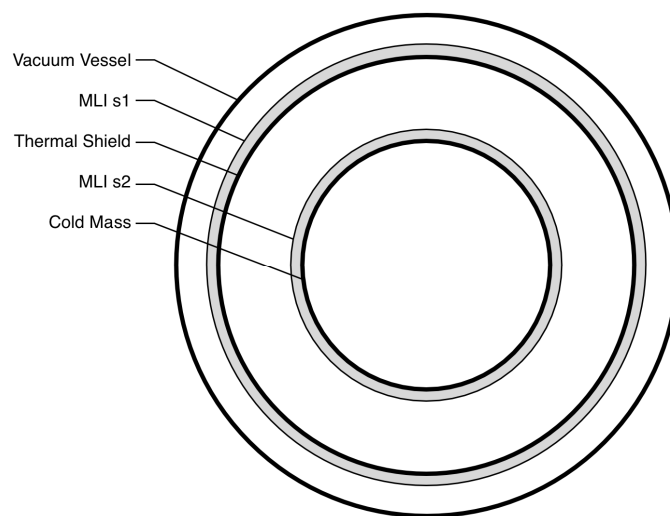
Fig. 1 - Cryostat one-dimensional radial model

Figure 1 shows the different heat transfer processes that have been taken into account for the development of the presented simulation tool. The mathematical model used to simulate them is detailed below.
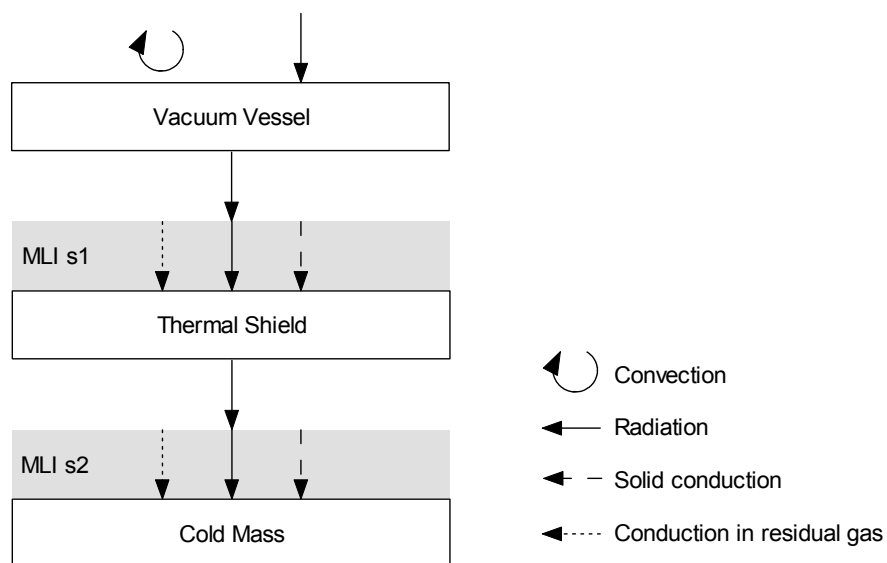
Fig. 2 - Heat in-leaks in a generic cryostat

2.2   Heat flux through MLI

Complete characterization of heat transfer through MLI is a quite difficult task because of several factors: coupled conduction and radiation heat transfer, temperature dependent physical properties, or complex geometries of the insulated system. For engineering design purposes, simpler procedures to evaluate the heat transfer rate through MLI are needed. There are several approaches: (i) some of them use some coefficients that are obtained experimentally and are specific for certain vacuum conditions and types of MLI [1,2]; (ii) others are focused on modeling the thermal behaviour of MLI under a wider range of situations; these approaches present an increased complexity, but are suitable for different types of MLI and pressure conditions [3].

There are several models of the heat transfer through MLI that follow the first approach (i) [4]. The following relationship considers the radiative and conductive effects:

$$\dot{q} = \frac{\alpha_S}{N_S} \frac{T_1 + T_2}{2} (T_1 - T_2) + \frac{\beta_S}{N_S} (T_1^4 - T_2^4) + \gamma_S P_S (T_1 - T_2) \tag{1}$$

where $\dot{q}$ is the heat flux in W/m^2, N_S is the number of layers in MLI blanket, T_1 and T_2 are the temperatures of the warm and cold surface respectively. The first term takes into account for solid conduction, the second for radiation, and the third for conduction in residual gas. The coefficient α_S is the average thermal conductivity of the reflective insulation system, and β_S is the average emissivity of MLI foils, and $\gamma_S = C_p/C_v$ is the ratio of specific heats and P_S is the residual gas pressure. At low residual gas pressure (10^{-4} Pa) conduction in residual gas can be neglected and heat transfer is only given by radiation and solid conduction. In this model, α_S and β_S must be obtained experimentally, for example, measuring the heat flux through MLI for two different temperature ranges (300-80 K and 80-4.5 K).

In the second approach (ii), to obtain a layer to layer MLI heat flux model it is necessary to take into account the heat transfer phenomena that occurs in-between its layers, which is shown in Fig. 3.
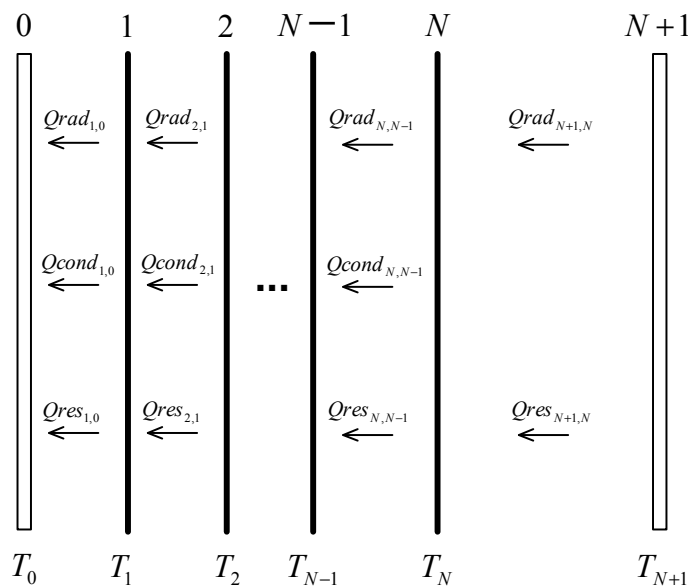

Fig. 3 - MLI layer-to-layer heat transfer scheme

The heat transfer through the MLI blanket can be then described by the following system of N+1 equations:

$$\dot{Q} = \dot{Q}rad_{2\rightarrow1} + \dot{Q}cond_{2\rightarrow1} + \dot{Q}res_{2\rightarrow1}$$
$$\dot{Q} = \dot{Q}rad_{3\rightarrow2} + \dot{Q}cond_{3\rightarrow2} + \dot{Q}res_{3\rightarrow2}$$
$$...\tag{2}$$
$$\dot{Q} = \dot{Q}rad_{N\rightarrow N-1} + \dot{Q}cond_{N\rightarrow N-1} + \dot{Q}res_{N\rightarrow N-1}$$
$$\dot{Q} = \dot{Q}rad_{N+1\rightarrow N} + \dot{Q}res_{N+1\rightarrow N}$$

where $\dot{Q}$ is the total heat transferred through the MLI blanket, $\dot{Q}rad_{i+1\rightarrow i}$ is the radiation from layer i+1 to layer i, $\dot{Q}cond_{i+1\rightarrow i}$ refers to solid conduction through the spacer between layer i+1 and layer i, $\dot{Q}res_{i+1\rightarrow i}$ is the residual gas conduction between two adjacent layers, and N is the number of layers in the MLI blanket.

In this layer-to-layer model of MLI there are at least three key physical phenomena to be studied: emissivity of shields, thermal conductivity of spacers, and residual gas pressure distribution in-between shields.

2.2.1   MLI shields emissivity

MLI shields are made with a material opaque to thermal radiation, Mylar or Kapton, coated with a thin and highly reflective layer of gold or aluminium. The thickness of this layer has to be kept at a minimum to minimise lateral thermal conduction.

The emissivity of a metal plate is temperature dependent. To estimate the emissivity of MLI shields it is necessary to obtain a temperature dependent form of it. This can be done using the Hagen-Rubens approximation, which is valid for radiation wavelengths longer than 5 microns. In the temperature range of 300 K to 4 K this approximation is valid, and the expression obtained is the following [14]:

$$\varepsilon(T) = k_1[\rho(T)\cdot T]^{0.5} + k_2\rho(T)\cdot T \qquad k_1 = 5.76 \qquad k_2 = 12.4 \tag{3}$$

where $\rho(T)$ is the temperature dependent electrical resistivity of the metal, which is at temperature T.

In the literature, there are many other expressions to estimate the emissivity of the MLI shield, but these solutions are valid only for a specific type and configuration of MLI, as they are fits to empirical data [1,2,15].

Figure 4 compares the estimated temperature dependent emissivity of Double Aluminized Mylar (DAM) shields using Hagen-Rubens approximation with several best fits found in the literature for the same type of MLI.

Equation 3 does not take into account the thermal emissivity of the spacers. But it can be neglected, as the density of the spacers usually is very small.
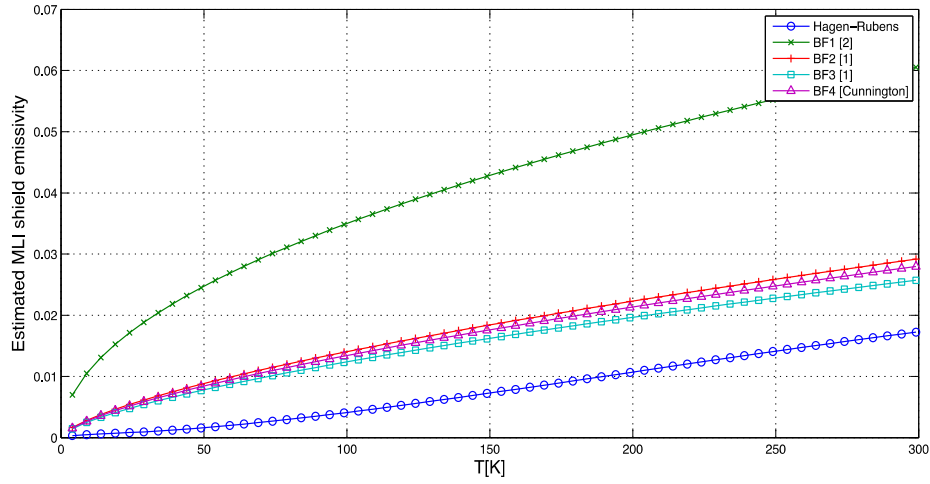
Fig. 4 - Temperature dependent emissivity of Double Aluminized Mylar (DAM) MLI shields

2.2.2   Spacers thermal conductivity

Heat transfer through the spacer material is one of the most complex phenomena to be model when analysing MLI behaviour. That is because the spacer material properties and the thermal contact resistance at the boundary between the spacer and the shield are very difficult to determine. This thermal contact, which depends on the assembly techniques used, is made only at a few discrete locations rather than over the entire surface area. Heat flow is constricted around the contact locations, and the presence of oxides on the surfaces in contact adds an additional variable to the conductance. Although extensive databases exist on the thermal properties of bulk materials, similar databases for pressed contacts do not.

Many researchers have made measurements of thermal contact resistance at cryogenic temperatures, but the data available in the literature is very limited. For standard spacer materials, the thermal conductivity varies from 1×10^{-6} to 1×10^{-3} W/m K (see Fig. 5) [21,2,20].
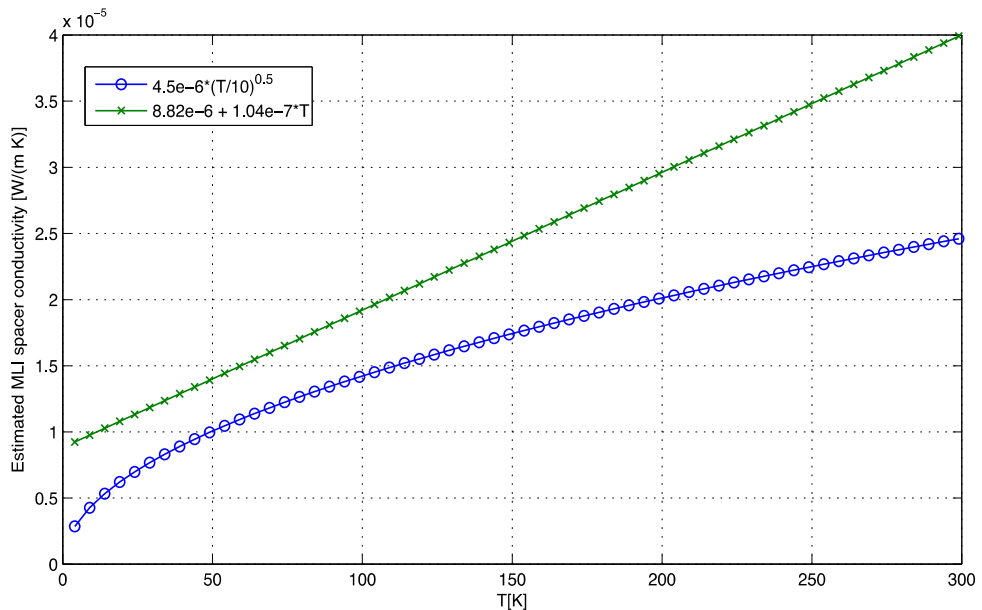

Fig. 5 - Temperature dependent thermal conductivity of typical MLI spacers

2.2.3   Interstitial gas pressure

Gas conduction between the shields usually falls into the free molecule regime as the mean free path of helium molecules at low temperature and low pressure is much bigger than the distance between shields. In this regime, heat transfer is basically due to collisions of molecules from one shield to the next one, so it is proportional to gas pressure in-between shields and to the accommodation coefficient of the gas to the plate material. At low pressure, a relationship developed by Kennard [17] can be used to estimate the heat transfer between concentric spheres, coaxial cylinders, or parallel plates and is as follows:

$$Q = A_1 \alpha \left(\frac{\gamma+1}{\gamma-1} \right) \left(\frac{R}{8\pi} \right)^{0.5} \frac{P}{(MT)^{0.5}} (T_2 - T_1) \tag{4}$$

$$\alpha = \frac{\alpha_1 \alpha_2}{\alpha_2 + \alpha_1 (1 - \alpha_2) A_1 / A_2} \tag{5}$$

where

Q is the heat received by surface A_1 in watts
α is the overall accommodation coefficient [18]
γ is c_p / c_v, the specific heat ratio of the gas, assumed constant
R is the molar gas constant
P is the pressure
M is the molecular weight of the gas
T is absolute temperature, which has a value intermediate between T_1 and T_2 but is not the average and subscripts 1 and 2 refer to the inner and outer surface, respectively.

At low temperatures, the accommodation coefficient becomes temperature dependent. Helium molecules in-between shields collide with molecules of other gases that stick to shields. In the literature there are few expressions to estimate the temperature dependent accommodation coefficient. In [14], the following expression is proposed to estimate $\alpha(T)$ of helium to an aluminium plate:

$$\alpha(T) = k_3 e^{-T/20} + k_4 T \qquad k_3 = 1.23 \qquad k_4 = 8.34 \times 10^{-4} \tag{6}$$

where T is the temperature of the plate. This equation is valid over the range of temperatures from 5 K to 500 K.

High MLI layer density and the outgassing process of MLI shields and spacer materials contribute to increase the interstitial gas pressure, which can be orders of magnitude higher than the pressure in the insulation vacuum space. Under certain conditions, interstitial gas pressure contribution to heat flux through MLI can be very important, this is why there are many works trying to model its distribution along the stack of MLI layers [19,14].

2.3   Specific heat

Most of the work on material properties at low temperatures was performed before the desktop computer became available. Data on specific heat or thermal conductivity at low temperatures are published in simple tables or graphically. It is really difficult to use this information in an accurate manner.

The US National Institute of Standards and Technology (NIST) began a program to gather cryogenic material property data and make it available in a form that is useful for engineers [5]. In their approach they use simple types of equations, such as polynomial or logarithmic polynomials, and determine the coefficients for different materials and properties. Engineers can now use these equations to predict material properties in a variety of ways.

In the case of specific heat, the ratio of the change in energy to the change in temperature, the general form of the equation used to predict its value is

$$\log(C_p) = a + b\log T + c(\log T)^2 + d(\log T)^3 + e(\log T)^4 + f(\log T)^5 + g(\log T)^6 + \\ + h(\log T)^7 + i(\log T)^8 \tag{7}$$

where a, b, c, d, e, f, g, h and i are the fitted coefficients and T is the temperature in Kelvin.

For the specific heat calculation of iron, which is also available in the simulation tool, a fitted curve to its graphical representation by NIST [6] was used. For the moment, there are no coefficients for Iron in NIST database [7].

Specific heat of helium has been numerically evaluated with HePAK [8].

2.4 Model

The model is based on a combination of theoretical analysis and empirical data. The empirical data is related with the heat transfer through MLI, which involves too complex phenomena for analytical analysis.

2.4.1 Vacuum Vessel

The vacuum enclosure at temperature T_{vv} receives heat from the tunnel wall at temperature T_{wall} by radiation and natural convection in air.

$$\dot{Q}_{rad_{vv}} = \sigma \overline{A}_{vv} E_1 (T^4_{wall} - T_{vv}^4) \tag{8}$$

$$\dot{Q}_{conv_{vv}} = h_C \overline{A}_{vv} (T_{wall} - T_{vv}) \tag{9}$$

where E_1 is the emissivity factor between the wall of the tunnel and the external surface of the vacuum vessel, and h_C is the natural convection heat transfer coefficient:

$$E_1 = \left(\varepsilon^{-1}{}_{vv} + \frac{A_{vv}}{A_{wall}} (\varepsilon^{-1}{}_{wall} - 1) \right)^{-1} \tag{10}$$

$$h_C = 1.3 \left(\frac{T_{wall}}{D_{vv}} \right)^{0.25} \tag{11}$$

The total heat reaching the vacuum vessel can be written as follows:

$$\dot{Q}_{w,vv} = \dot{Q}_{rad_{vv}} + \dot{Q}_{conv_{vv}} \qquad (12)$$

2.4.2 Thermal shield

The outer layer of superinsulation that covers the thermal shield (s1) at temperature T_{s1} receives heat from the vacuum vessel at temperature T_{vv} by radiation.

$$\dot{Q}_{vv,s1} = \dot{Q}_{rad_{vv,s1}} = \sigma \overline{A}_{s1} E_2 (T^4{}_{vv} - T_{s1}{}^4) \qquad (13)$$

where E_2 is the emissivity factor between the vacuum vessel and the outer layer of superinsulation (s1):

$$E_2 = \left(\varepsilon^{-1}{}_{s1} + \frac{A_{s1}}{A_{vv}} (\varepsilon^{-1}{}_{vv} - 1) \right)^{-1} \qquad (14)$$

2.4.3 Heat transfer through MLI (30 layers)

Heat transfer to the thermal shield through the superinsulation system is given by radiation between reflective layers, solid conduction through spacers and conduction in residual gas. At low residual gas pressure (10^{-4} Pa) conduction in residual gas can be neglected and heat transfer is only given by radiation and solid conduction [9].

$$\dot{Q}_{rad_{s1}} = \overline{A}_{ts} \frac{\beta_S}{N_{s1}} (T_{s1}{}^4 - T_{ts}{}^4) \qquad (15)$$

$$\dot{Q}_{sc_{s1}} = \overline{A}_{ts} \frac{\alpha_S}{N_{s1}} \left(\frac{T_{s1} + T_{ts}}{2} \right) (T_{s1} - T_{ts}) \qquad (16)$$

where α_S and β_S are the average thermal conductivity and emissivity constants of the superinsulation system (obtained experimentally) and N_{s1} is the number of reflective layers.

$\alpha_S = 1.401 \cdot 10^{-4}$ [W/m^{2}K^2]   (at 10^{-4} Pa)

$\beta_S = 3.741 \cdot 10^{-9}$ [W/m^{2}K^4]   (at 10^{-4} Pa)

$N_{s1} = 30$

The total heat transfer through MLI can be written as follows:

$$\dot{Q}_{s1,ts} = \dot{Q}_{rad_{s1}} + \dot{Q}_{sc_{s1}} = \dot{Q}_{vv,s1} \qquad (17)$$

It is possible to calculate the temperature of the outer layer of MLI s1 (T_{s1}) by solving Eq. (17).

2.4.4   Cold mass

The outer layer of superinsulation (s2) on the cold mass at temperature T_{s2} receives heat from the thermal shield at temperature T_{ts} by radiation.

$$\dot{Q}_{ts,s2} = \sigma \overline{A}_{s2} E_3 (T^4{}_{ts} - T_{s2}{}^4) \qquad (18)$$

where E_3 is the emissivity factor between the thermal shield and the outer layer of superinsulation (s2):

$$E_3 = \left(\varepsilon^{-1}{}_{s2} + \frac{A_{s2}}{A_{ts}} (\varepsilon^{-1}{}_{ts} - 1) \right)^{-1} \qquad (19)$$

2.4.5   Heat flux through MLI on cold mass

Heat transfer to the cold mass through superinsulation system is given by radiation between reflective layers, solid conduction through spacers and conduction in residual gas. As the residual gas pressure is low (10^{-4} Pa) conduction in residual gas can be neglected.

$$\dot{Q}_{rad_{s2}} = \overline{A}_{s2} \frac{\beta_S}{N_{s2}} (T_{s2}{}^4 - T_{cm}{}^4) \qquad (20)$$

$$\dot{Q}_{sc2} = \overline{A}_{s2} \frac{\alpha_S}{N_{s2}} \left(\frac{T_{s2} + T_{cm}}{2} \right) (T_{s2} - T_{cm}) \qquad (21)$$

where

$\alpha_S = 1.401 \cdot 10^{-4}$ [W/m^{2}K^2]   (at 10^{-4} Pa)

$\beta_S = 3.741 \cdot 10^{-9}$ [W/m^{2}K^4]   (at 10^{-4} Pa)

$N_{s2} = 10$

Finally, total heat transfer from the outer layer of superinsulation s2 to the cold mass can be written as:

$$\dot{Q}_{s2,cm} = \dot{Q}_{rad_{s2}} + \dot{Q}_{sc_{s2}} = \dot{Q}_{ts,s2} \qquad (22)$$

As in the previous section, it is possible to calculate the temperature of the outer layer of MLI s2 (T_{s2}) by solving Eq. (22).

2.4.6   Complete model

Applying the law of conservation of energy to the vacuum vessel, thermal shield and cold mass, we obtain a system of five differential equations from which we calculate T_{vv}, T_{s1}, T_{ts}, T_{s2} and T_{cm}:

$$M_{vv} C_{p_{vv}}(T_{vv}) \frac{\partial T_{vv}}{\partial t} = \dot{Q}_{w,vv}(T_{vv}) - \dot{Q}_{vv,s1}(T_{vv}, T_{s1}) \tag{23}$$

$$M_{ts} C_{p_{ts}}(T_{ts}) \frac{\partial T_{ts}}{\partial t} = \dot{Q}_{s1,ts}(T_{s1}, T_{ts}) - \dot{Q}_{ts,s2}(T_{ts}, T_{s2}) \tag{24}$$

$$M_{cm} C_{p_{cm}}(T_{cm}) \frac{\partial T_{cm}}{\partial t} = \dot{Q}_{s2,cm}(T_{s2}, T_{cm}) \tag{25}$$

$$\dot{Q}_{vv,s1} = \dot{Q}_{s1,ts} \tag{26}$$

$$\dot{Q}_{ts,s2} = \dot{Q}_{s2,cm} \tag{27}$$

where M represents the mass per unit length in kg/m, and C_p is the specific heat in J/(kg K), whose value depends on the material in which each component of the cryostat is built of.

3   Case of study: model of LHC cryostat

In order to validate the presented mathematical model, a comparison between data obtained from the temperature sensors in the LHC and simulated results has been made. Table 1 shows the masses, main dimensions and materials used as inputs in the mathematical model for a simulation period of 55 days. These inputs correspond to a typical LHC dipole cryostat [22].

Table 1 - Masses, main dimensions and materials used in the simulated LHC model

	Vacuum vessel	Thermal shield	Cold mass
Materials	Iron	1100 Al/6061 Al	Iron/304 StSt/Cu/He
Diameter (m)	0.914	0.780	0.570
Mass (kg/m)	238.3	27.6	1998
Number of MLI layers	-	30	10
MLI spacer thickness (m)	-	0.0003	0.0003
Initial Temperature value (K)	294	65	2

Figure 6 shows the simulated evolution of the cold mass temperature of a LHC cryostat over time during a natural warm-up versus real temperature data registered by temperature sensors of such accelerator. The estimated temperature profile of the cold mass is in good agreement with the data from LHC in the first 10 days. From day 10 to 30 the agreement is only within 50% due to some variations in the observed temperature profile, possibly because of some maintenance operations that are not typical in a natural warm-up. From day 30 to 50 is within 20%. It is difficult to find temperature data of complete natural warm-ups of LHC cryostats. Data shown in Fig. 6 corresponds to partial natural warm-ups of sectors for different periods of time[1]. In particular, these warm-ups correspond to cold masses LBARA_12L8 and

---

[1] The chosen natural warm-up of sectors 7-8 and 8-1 starts on March 29 and ends on May 22, 2009.

LBALA_18R8 respectively. Data was taken from Timber [10] interface with one day frequency in scale down average mode.
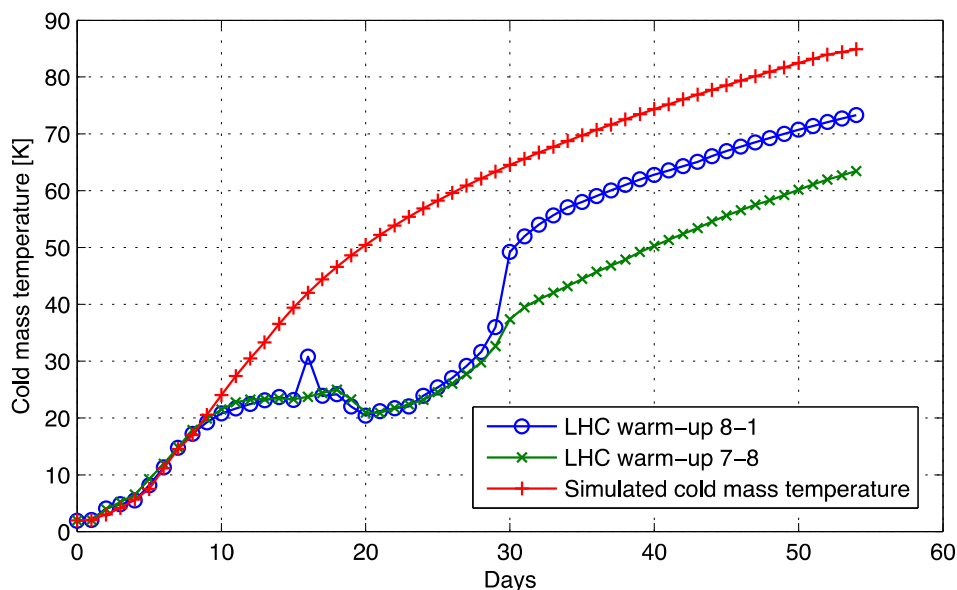

Fig. 6 - Simulated cold mass temperature during a natural warm-up

4 Thermal transients simulation tool

4.1 Model implementation

The mathematical model presented in Section 2.4 has been implemented using Matlab language. Two applications have been developed: MLIGUI and CryoModel. MLIGUI implements a layer-to-layer model of MLI and can be used to study the thermal performance of the insulation system for different configurations. CryoModel is a tool to simulate the evolution of the temperatures of different components of a generic cryostat during a natural warm-up.

4.2 MLIGUI

MLIGUI is an end-user tool that can be used without any Matlab programming knowledge. It provides a user-friendly GUI with several panels to guide the user while configuring several parameters for the heat flux through MLI calculation.

In order to estimate the heat flux through MLI for several configurations, a very simple model has been used. It consists of two concentric cylinders. The inner cylinder is considered as the cold boundary and MLI rests on it, while the external cylinder represents the hot boundary. Heat flows from the warm boundary to the cold one by radiation, conduction in residual gas, and solid conduction through MLI spacers. It is assumed that vacuum in-between cylinders is good, so there is no heat transfer by convection.

4.2.1 Geometry panel

In the geometry panel, the user defines the dimensions of the two concentric cylinders: hot boundary diameter (external cylinder) and cold boundary diameter (inner cylinder) (see Fig. 7).
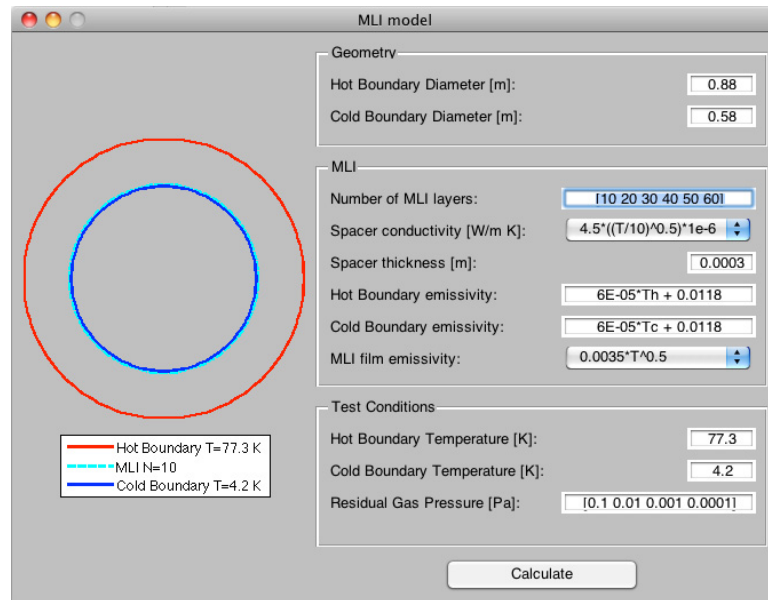
Fig. 7 - A view of MLIGUI application

4.2.2 MLI panel

All the parameters related with the MLI configuration are located in the MLI panel:

i) Number of MLI layers: it is possible to define one or several MLI setups with different number of layers. This is useful to compare the heat flux through MLI depending on the number of layers. Values are introduced as a Matlab row vector. For example, to define three MLI setups with 10, 20 and 30 layers respectively, the row vector [10 20 30] should be entered.

ii) Spacer conductivity: effective thermal conductivity of MLI spacer material in W/mK. User can choose between a set of two predefined effective conductivity expressions [2,20].

iii) Spacer thickness: individual spacer net thickness in meters.

iv) Hot boundary emissivity: it is possible to define either a function or a fixed value for the thermal emissivity of the hot boundary surface. In case of using a function, the variable *Th* represents the hot boundary surface temperature.

v) Cold boundary emissivity: in this case, the variable representing the cold boundary surface temperature is *Tc*.

vi) MLI film emissivity: the user can choose between a set of two predefined MLI film thermal emissivity expressions [1,2].

4.2.3 Test conditions panel

In this panel, test conditions like temperature and residual gas pressure are defined:

i) Hot boundary temperature: temperature of the hot boundary (external cylinder) in Kelvin.

ii) Cold boundary temperature: temperature of the cold boundary (inner cylinder) in Kelvin.

iii)   Residual gas pressure: vacuum pressure in-between cylinders in Pascal. It is possible to define several test cases by varying the residual gas pressure. For example, to define four test cases with a vacuum pressure of 0.1, 0.01, 0.001, and 0.0001 Pa the Matlab row vector [0.1 0.01 0.001 0.0001] should be entered.

4.2.4   Simulation results

When the thermal flux through MLI calculation for all the test cases, a new window opens with the results. Results are shown graphically in two plot areas (see Fig. 8). The first plot shows the total heat flux through MLI for the given boundary temperatures and different configurations (number of layers, residual gas pressure). It is possible to plot total heat flux either versus the number of MLI layers or versus residual gas pressure by checking N or P respectively in the X-axis data panel next to the plot area. There is also the possibility of plotting only one test case by selecting the appropriate value for N or P in the select boxes next to the plot area. The second plot shows, by default, the temperature of the surface of each MLI layer for different residual gas pressure configurations. By checking Q in the Y-axis data panel next to the plot area, the plot change and shows the layer-to-layer heat transfer for a given residual gas pressure test case. In both cases, it is possible to select a specific test case by using N and P select boxes next to the plot area.

View Data buttons open a window with the selected results presented in a table view. Export to CSV buttons generate a CSV file with the selected results for further analysis.
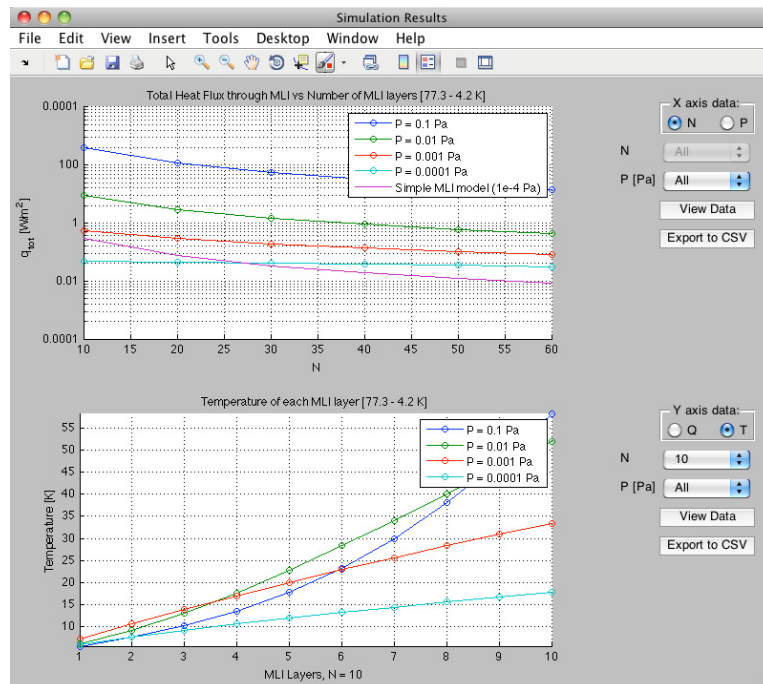

Fig. 8 - MLIGUI simulation results

4.3   CryoModel

The interactive application, CryoModel, is an end-user tool that can be used without any Matlab programming knowledge.

CryoModel simulation tool consist of two well-differentiated parts:

i)   a set of Matlab functions used to solve the system of equations described in Section 2.4;

ii)   a Graphical User Interface (GUI) developed also in Matlab to guide the user while configuring the generic cryostat parameters before launching the thermal transient simulation process, and to view or export its results (see Fig. 9).
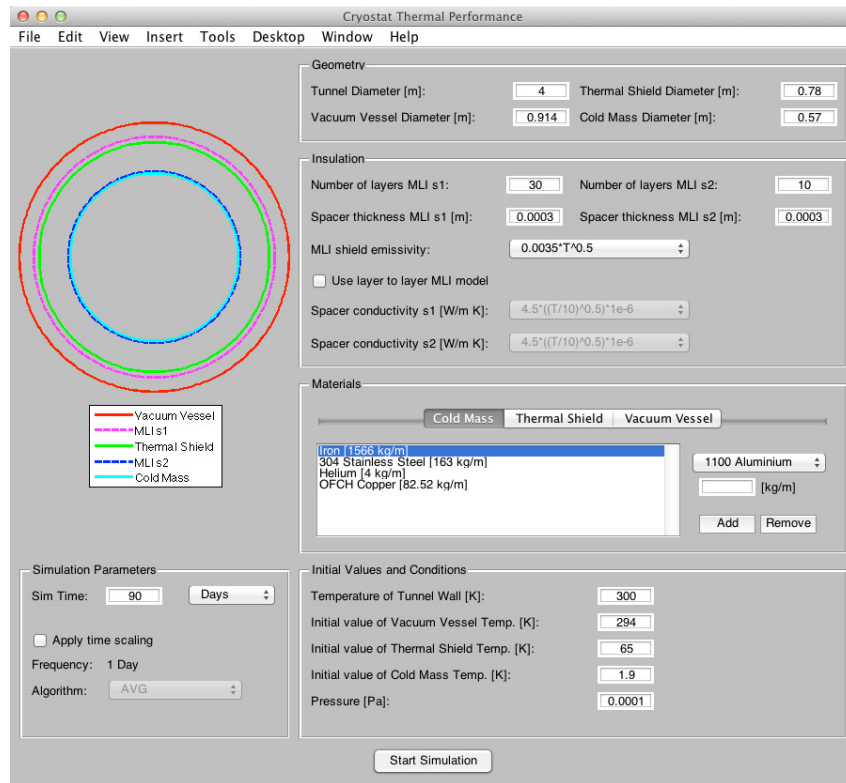

Fig. 9 - A view of CryoModel application

4.3.1   Geometry panel

In the geometry panel, the user can specify those cryostat model parameters that relate to its geometry:

i)   Tunnel Diameter: diameter in meters of the inner wall of the tunnel in which the cryostat is located.

ii)   Vacuum Vessel Diameter: diameter in meters of the vacuum vessel.

iii)   Thermal Shield Diameter: diameter in meters of the thermal shield.

iv)   Cold Mass Diameter: diameter in meters of the cold mass assembly.

4.3.2   Insulation panel

All the parameters related with the insulation system configuration are located in the insulation panel:

i)   Number of layers MLI s1: total number of shields in MLI blanket covering the thermal shield.

ii)   Number of layers MLI s2: total number of shields in MLI blanket covering the cold mass assembly.

iii)   Spacer thickness MLI s1: spacer thickness in meters of MLI covering the thermal shield.

iv)   Spacer thickness MLI s2: spacer thickness in meters of MLI covering the cold mass.

v)   MLI shield emissivity: the user can choose between a set of two predefined MLI film thermal emissivity expressions [1,2].

vi)   Use layer to layer MLI model: if this option is checked, the simulator will use a more detailed thermal model of MLI instead of the simpler model, which is limited to certain vacuum conditions and to a specific type of MLI (see Section 2.2).

vii)   Spacer conductivity s1: effective spacer material thermal conductivity of MLI covering the thermal shield in W/mK. User can choose between a set of two predefined effective conductivity expressions [2,20]. Only applicable if the layer to layer MLI model is selected.

viii)   Spacer conductivity s2: effective spacer material thermal conductivity of MLI covering the cold mass in W/mK. Only applicable if the layer to layer MLI model is selected.

4.3.3   Materials panel

In the materials panel, the user defines the materials and masses per unit length of the different components of the cryostat. There are three tabs, one per each cryostat component: vacuum vessel, thermal shield and cold mass. In each tab, there is a list of pre-built materials from which the user can choose and an input text to indicate its weight in kg/m. Each component can be composed by one material or by a combination of several materials.

4.3.4   Simulation parameters panel

The simulation time and the time scaling algorithm (if any) to be used in the simulation results are configured in the simulation parameters panel. Due to the Ordinary Differential Equations (ODE) solver used to find the solution to the system of equations presented in section 2.4.6, the simulation results are asynchronous. To have the results at a given moment in time, there is the option to apply a time scaling algorithm to these results. The time scaling algorithms currently implemented are MIN, MAX and AVG. These algorithms derives values at the chosen interval frequency by truncating the timestamps of the simulated time series data to the start times of the derived intervals, and then calculate the minimum (MIN), maximum (MAX) or average (AVG) value of the simulation results in that time interval.
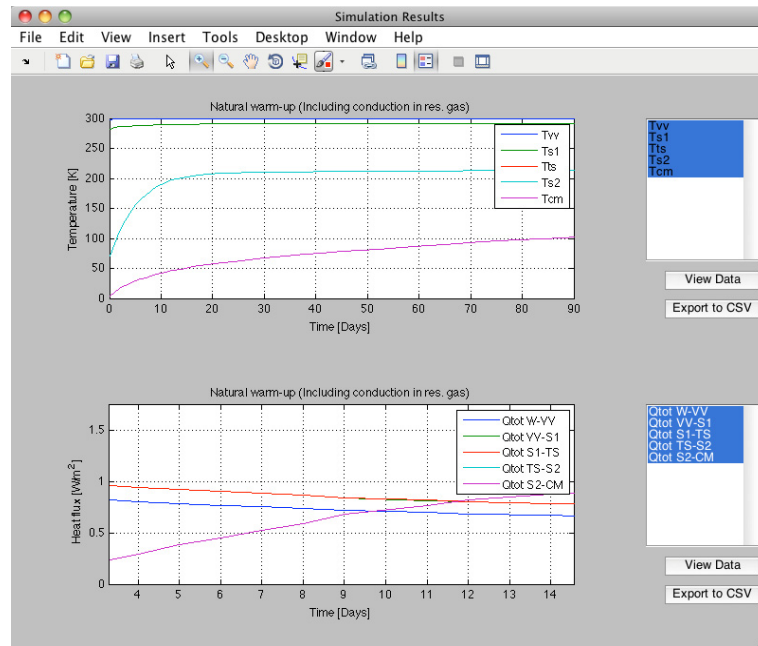
Fig. 10 - Simulation results

4.3.5   Initial values and conditions panel

In this panel, the user defines the initial values of different variables needed for the simulation of thermal transients in the cryostat:
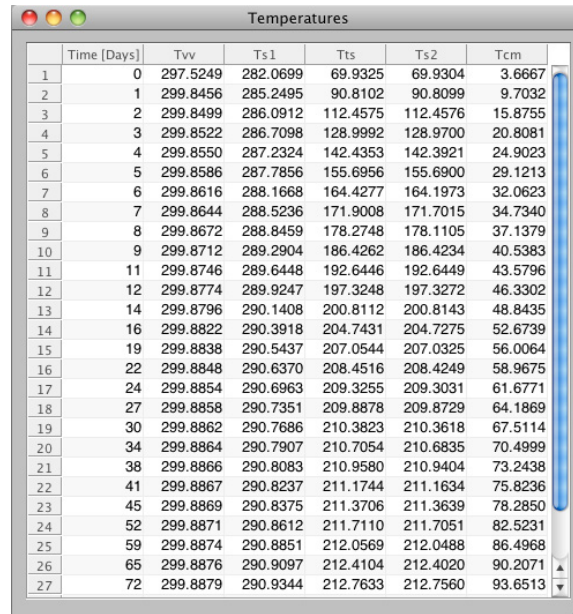
i)   Temperature of tunnel wall: temperature in Kelvin of the inner wall of the tunnel in which the cryostat is located. This temperature is considered as a constant; its value does not change during the simulation.

ii)   Initial value of vacuum vessel temperature in Kelvin.

iii)   Initial value of thermal shield temperature in Kelvin.

iv)   Initial value of cold mass temperature in Kelvin.

v)   Pressure: vacuum pressure inside the cryostat in Pascal.

4.3.6   Simulation results

When simulation process ends, results are shown in a new window. It is possible to see the results either graphically or numerically, as well as to export them in a CSV file for further analysis (see Fig. 10-Fig. 11).

By default, results are shown graphically using two plot areas as shown in Fig. 10. The first one shows the evolution in time of a set of temperatures: vacuum vessel temperature (Tvv), outer layer temperature of MLI on the thermal shield ($Ts1$), thermal shield temperature (Tts), outer layer temperature of MLI on the cold mass ($Ts2$), cold mass temperature (Tcm). It is possible to plot only one, or several, of these temperatures by selecting them in the list next to the plot area. Clicking on the View Data button opens a new window with the selected temperature data presented in a table view (see Fig. 11). Export to CSV button generates a CSV file with selected temperature data. The second plot shows the evolution in time of the heat flux through the cryostat divided in five stages: total heat flux from tunnel wall to vacuum vessel ($Qtot$ W-VV), total heat flux from vacuum vessel to outer layer of MLI on thermal shield

(*Qtot* VV-S1), total heat flux through MLI on thermal shield (*Qtot* S1-TS), total heat flux from thermal shield to outer layer of MLI on cold mass (*Qtot* TS-S2), total heat flux through MLI on cold mass (*Qtot* S2-CM). As the previous plot, it is possible to configure the total heat fluxes to be plot by selecting them in the list next to the plot area. Clicking on the View Data button opens a new window with the selected total heat flux data presented in a table view. Export to CSV button generates a CSV file with selected total heat flux data.

	Time [Days]	Tvv	Ts1	Tts	Ts2	Tcm
1	0	297.5249	282.0699	69.9325	69.9304	3.6667
2	1	299.8456	285.2495	90.8102	90.8099	9.7032
3	2	299.8499	286.0912	112.4575	112.4576	15.8755
4	3	299.8522	286.7098	128.9992	128.9700	20.8081
5	4	299.8550	287.2324	142.4353	142.3921	24.9023
6	5	299.8586	287.7856	155.6956	155.6900	29.1213
7	6	299.8616	288.1668	164.4277	164.1973	32.0623
8	7	299.8644	288.5236	171.9008	171.7015	34.7340
9	8	299.8672	288.8459	178.2748	178.1105	37.1379
10	9	299.8712	289.2904	186.4262	186.4234	40.5383
11	11	299.8746	289.6448	192.6446	192.6449	43.5796
12	12	299.8774	289.9247	197.3248	197.3272	46.3302
13	14	299.8796	290.1408	200.8112	200.8143	48.8435
14	16	299.8822	290.3918	204.7431	204.7275	52.6739
15	19	299.8838	290.5437	207.0544	207.0325	56.0064
16	22	299.8848	290.6370	208.4516	208.4249	58.9675
17	24	299.8854	290.6963	209.3255	209.3031	61.6771
18	27	299.8858	290.7351	209.8878	209.8729	64.1869
19	30	299.8862	290.7686	210.3823	210.3618	67.5114
20	34	299.8864	290.7907	210.7054	210.6835	70.4999
21	38	299.8866	290.8083	210.9580	210.9404	73.2438
22	41	299.8867	290.8237	211.1744	211.1634	75.8236
23	45	299.8869	290.8375	211.3706	211.3639	78.2850
24	52	299.8871	290.8612	211.7110	211.7051	82.5231
25	59	299.8874	290.8851	212.0569	212.0488	86.4968
26	65	299.8876	290.9097	212.4104	212.4020	90.2071
27	72	299.8879	290.9344	212.7633	212.7560	93.6513

Fig. 11 - Simulation results. Table view

4.3.7   Add/remove thermal conductivity expressions

Thermal conductivity expressions are coded in *conductivity_calc.m* Matlab file that is located in *materials* folder.

In order to add a new thermal conductivity expression it is necessary to create a new case in the switch statement inside *conductivity_calc* function with the new expression. The variable *T* represents the temperature in Kelvin of the material, and *ks* is its thermal conductivity.

5   Conclusion and future work

The understanding of thermal transients is important in the design process of any cryostat to estimate downtime for intervention. To study these transient modes, a one-dimensional radial model of a generic cryostat has been developed. This model consists of a cold mass, a thermal shield and a vacuum vessel. Blankets of MLI covering the thermal shield and the cold mass have also been considered in this model. Modeling the heat flux through the insulation system is a quite difficult task and it is actually under research. In the presented model, two different approaches to thermal modeling of MLI have been used.

Two Matlab applications have been developed: MLIGUI and CryoModel. Both of them implement a user-friendly GUI and are multiplatform. MLIGUI can be used to estimate the heat flux and individual layer temperatures for different MLI configurations. CryoModel simulates the evolution of the temperature over time of the main components of a generic cryostat during a natural warm-up.

The results obtained with the CryoModel tool have been benchmarked on temperature data from transients of the LHC. Some improvements should be made in the mathematical model and in the simulation tool to improve its accuracy. The proposed future work is:

- Interface HePAK application with the simulation tool in order to get more precise values for Helium specific heat depending on pressure and temperature.

- Vacuum conditions in the cryostat are supposed to be good enough to neglect heat transfer by convection. A possible improvement in the model is to add this heat transfer mechanism to be able to study a wider range of vacuum conditions.

- In the current model the vacuum pressure inside the cryostat is assumed to be constant. It would be interesting to have the possibility to introduce variable pressure conditions, which would affect the heat transfer by convection inside the cryostat.

- Static heat in-leaks coming from the support posts or electrical feedthroughs are not actually considered in the presented model.

- Include the option of having an actively cooled thermal shield and calculate its refrigeration power.

- Develop more transient modes like forced warm-up or cool-down.

Acknowledgement

References

[1] T.C. Nast, D.J. Frank, and I.E. Spradley, Investigations of multilayer insulation at low boundary temperatures, ICEC-11, 1986.

[2] M. Chorowski, P. Grzegory, C. Parente, and G. Riddone, Optimisation of multilayer insulation - An engineering approach, LHC Project Report 464, 2001.

[3] M. Chorowski, P. Grzegory, C. Parente, and G. Riddone, Experimental and mathematical analysis of multilayer insulation below 80 K, CERN, 2000.

[4] C.K. Krishnaprakas, K.B. Narayana, and P. Dutta, Heat transfer correlations for multilayer insulation systems, Cryogenics 40 (2000), p. 431-435.

[5] E.D. Marquardt, J.P. Le, and R. Radebaugh, Cryogenic material properties database, Proc. IEEE 11th International Cryocooler Conf., 2000.

[6] R.B. Stewart, A compendium of the properties of material at low temperature, Phase II, Technical Report, WADD, 1961.

[7] NIST, Cryogenic Material Properties. http://cryogenics.nist.gov/MPropsMAY/materialproperties.htm (accessed 09 27, 2010).

[8] Cryodata Inc., User's Guide to HePAK Version 3.4. 1999.

[9] G. Riddone, Theoretical modeling and experimental investigation of the thermal performance of the LHC lattice cryostats, PhD Thesis, Turin Polytechnic, 1997.

[10] CERN, LHC Logging Project. http://lhc-logging.web.cern.ch/lhc-logging (accessed 09 27, 2010).

[11] GridBagLayout, http://www.mathworks.com/matlabcentral/fileexchange/22968-gridbaglayout (accessed 03 21, 2011).

[12] T.H. Nicol, C. Darve, Y. Huang, and T.M. Page, LHC Interaction Region Quadrupole Cryostat Design and Fabrication, IEEE Trans. on Applied Superconductivity, 2002, Vol. 12, p. 179-182

[13] M. Castoli, M. Pangallo, V. Parma, and G. Vandoni, Thermal performance of the supporting system for the Large Hadron Collider (LHC) superconducting magnets, LHC Project Report 335, 1999.

[14] M.A. Green, Radiation and gas conduction heat transport across a helium Dewar multilayer insulation system, Lawrence Berkeley Laboratory, Berkeley, 1994.

[15] G.R. Cunnington, C.W. Keller, and G.A. Bell, Thermal performance of multilayer insulations, Interim report, Lockheed Missiles & Space Company, Sunnyvale, California, 1971.

[16] R.R. Conte, Eléments de cryogénie (Masson, Paris, 1970).

[17] E.H. Kennard, Kinetic theory of gases, McGraw-Hill Book Co., 1938.

[18] R.J. Corruccini, Gaseous heat conduction at low pressures and temperatures, Vacuum, Vol. VII&VIII, 1959.

[19] J. Polinski, Cryostat for thermal measurements of cryogenic insulations with evaporative method, Multiconference CryoPrague 2006 (9th Cryogenics 2006, ICEC 21, ICMC'06).

[20] J. Polinski, M. Chorowski, A. Choudhury, T.S. Datta, Synthesis of the multilayer cryogenic insulation modelling and measurements, Advances in Cryogenic Engineering: Transactions of the Cryogenic Engineering Conference, CEC, Vol. 53, 2008.

[21] L.J. Salerno, P. Kittel, Thermal Contact Conductance, NASA Technical Memorandum 110429, 1997.

[22] O.S. Brüning, P. Collier, P. Lebrun, S. Myers, R. Ostojic, J. Poole, P. Proudlock, LHC Design Report, CERN, Geneva, 2004.

Appendix A: MLIGUI

A.1 File Structure

The following directories and files comprise the MLIGUI simulation tool:

+layout/

This contains the GridBagLayout class files. layout.GridBagLayout [11] is a Matlab class which controls layout and resize of a figure/uipanel/uicontainer. This class helps the Matlab GUI developer design complex GUI without the need for calculations or complex code for performing initial layouts or writing resize functions.

materials/

Includes Matlab function files related with material properties calculation like the specific heat, the thermal emissivity or the thermal conductivity.

MLIGUI_distrib/

Includes the redistributable packages needed to run MLIGUI as a standalone application in different operating systems.

utils/

This folder contains utility function files like implode/explode or the time scaling algorithms.

MLIGUI.m

Main source file of the simulation application.

MLIparam.m

This file concentrates all the configurable parameters and initial values needed for the MLI heat flux and layer temperature calculations.

MLIModel.m

It contains layer-to-layer heat flux through MLI model implementation.

MLI.m

This function implements the necessary system of equations to estimate heat flux through MLI. It calls MLIModel.m.

english.xml

English language file for MLIGUI.

A.2 Running MLIGUI as a standalone application

Windows Operating System

Run self-extracting package MLIGUI_Windows.exe

This package contains:
MLIGUI.exe
MCRInstaller.exe
Readme file

If the MATLAB Compiler Runtime (MCR) is not installed, MCRInstaller.exe will install it automatically. MCR is a standalone set of shared libraries that enable the execution of M-files. The MCR provides complete support for all features of MATLAB without the MATLAB GUI.

Once the MCR has been installed, the main application can be run by executing the file MLIGUI.exe.

OSX

Run MCRInstaller.dmg to install the MATLAB Compiler Runtime (MCR).

Once the MCR has been installed, the main application can be run simply by executing the file MLIGUI.app.

GNU/Linux

Run MCRInstaller.bin to install the MATLAB Compiler Runtime (MCR).

Once the MCR has been installed, the main application can be run simply by executing the file MLIGUI

Appendix B: CryoModel

B.1 File Structure

The following directories and files comprise the CryoModel simulation tool:

+layout/

> This contains the GridBagLayout class files. layout.GridBagLayout [11] is a Matlab class which controls layout and resize of a figure/uipanel/uicontainer. This class helps the Matlab GUI developer design complex GUI without the need for calculations or complex code for performing initial layouts or writing resize functions.

+splashscreen/

> This folder includes function files and images needed to create the splash screen of the application.

CryoModel_distrib/

> Includes the redistributable packages needed to run CryoModel as a standalone application in different operating systems.

materials/

> Includes Matlab function files related with material properties calculation like the specific heat, the thermal emissivity or the thermal conductivity.

utils/

> This folder contains utility function files like implode/explode or the time scaling algorithms.

CryoModel.m

> Main source file of the simulation application.

config.m

> This file concentrates all the configurable parameters and initial values needed for the thermal transient simulation to run.

CryoSimSimple.m

> This function implements the system of equations presented in Section 2.4.6. It employs the engineering approximation described in Section 2.2 to estimate heat flux through MLI.

CryoSim.m

> This file contains the implementation of the system of equations presented in Section 2.4.6. It employs the layer-to-layer heat flux through MLI model for the simulation.

CryoSimOutFcn.m

This file is called by MLI_model function. Its mission is to store final results of ODE solver at the end of each simulation iteration in order to plot them when the simulation ends.

MLIModel.m

It contains layer-to-layer heat flux through MLI model implementation.

B.2 Running CryoModel as a standalone application

Windows Operating System

Run self-extracting package CryoModel_Windows.exe

This package contains:
CryoModel.exe
MCRInstaller.exe
Readme file

If the MATLAB Compiler Runtime (MCR) is not installed, MCRInstaller.exe will install it automatically. MCR is a standalone set of shared libraries that enable the execution of M-files. The MCR provides complete support for all features of MATLAB without the MATLAB GUI.

Once the MCR has been installed, the main application can be run simply by executing the file CryoModel.exe.

OSX

Run MCRInstaller.dmg to install the MATLAB Compiler Runtime (MCR).

Once the MCR has been installed, the main application can be run simply by executing the file CryoModel.app.

GNU/Linux

Run MCRInstaller.bin to install the MATLAB Compiler Runtime (MCR).

Once the MCR has been installed, the main application can be run simply by executing the file CryoModel